

Chapter 1. Global agroclimatic patterns

Chapter 1 describes the CropWatch Agroclimatic Indicators (CWAIs) rainfall (RAIN), temperature (TEMP), and radiation (RADPAR), along with the agronomic indicator for potential biomass (BIOMSS) in sixty-five global Monitoring and Reporting Units (MRU). Rainfall, temperature, and radiation indicators are compared to their average value for the same period over the last fifteen years (called the “average”), while BIOMSS is compared to the indicator’s average of the recent five years. Indicator values for all MRUs are included in Annex A table A.1. For more information about the MRUs and indicators, please see Annex C and online CropWatch resources at www.cropwatch.com.cn.

1.1 Introduction

A statistical analysis of table A.1 (CWAIs by CropWatch MRU) does not highlight any marked connections between CWAIs (RAIN, TEMP, RADPAR, and BIOMSS) apart from those expected from climatology: higher temperatures in high rainfall (that is, equatorial) areas compared with temperate zones. Other parallel variations include the changes in RADPAR and temperature and, because of the model used, BIOMSS and RAIN. One interesting observation, however, involves TEMP departures, which tend to be negative in high rainfall areas, meaning that tropical areas generally tended to experience below average TEMP.

As a reminder: CropWatch agroclimatic indicators are computed only over agricultural areas (with additional weighting to highlight the most productive areas), while non-agricultural areas are not included in the averaging process. Moreover, where large spatial intra-MRU climatic variations occur, this is usually visible from the higher resolution national and sub-national data described in Chapter 3.1, not to mention the national analyses in Chapters 3 and 4. Note also that the MRUs only have been given names for easy reference; these names do not, generally, correspond with existing political entities (such as for example in the case of the "Eastern Central Asia" MRU (MRU-52).

1.2 Rainfall (RAIN)

Among the locations that do expect significant rainfall during the reporting period (“significant” is somewhat arbitrarily put at 150 mm over the 4 months from April to July), the largest deficits occurred in Oceania and in Africa. In Australia, three MRUs deserve mentioning: MRU-54 (Queensland to Victoria) where rainfall was 32% below the expected amount of 168 mm, and Nullarbor to Darling (MRU-55), where the recorded amount of 94 mm was 57% below average. This MRU in fact experienced the worst departure in the CropWatch RAIN indicator of the current reporting period. In New-Zealand (MRU-56) the rainfall deficit is put at 29% (223 mm instead of 315).

In the lowlands of the Horn of Africa (HoA, MRU-04), measured rainfall reached 129 mm, 32% below the expected amount of 189 mm. As described in the focus section (Chapter 5) of this bulletin, the HoA suffered the third consecutive rainfall deficit season, resulting in severe hardship for people, animals and, crops. The neighboring highlands of East Africa (MRU-02) suffered a more moderate deficit (RAIN, -13%) which, combined with mostly high rainfall amounts (average above 50 mm) led to no serious consequences. MRU-02 and MRU-04 are shown as J in the summary figure 1.5.

Still significant--considering the scale of the MRUs--deficits are reported from eastern Asia (MRU-43, RAIN, -26%) and southern Japan and Korea (MRU-46, -30%). The area is indicated as I in figure 1.5.

RAIN deficit areas also include the Brazilian Nordeste (MRU-22 with RAIN, -26%) and the Southwestern Southern Cone (Western Patagonia, MRU-27), which recorded 328 mm instead of 469 mm.

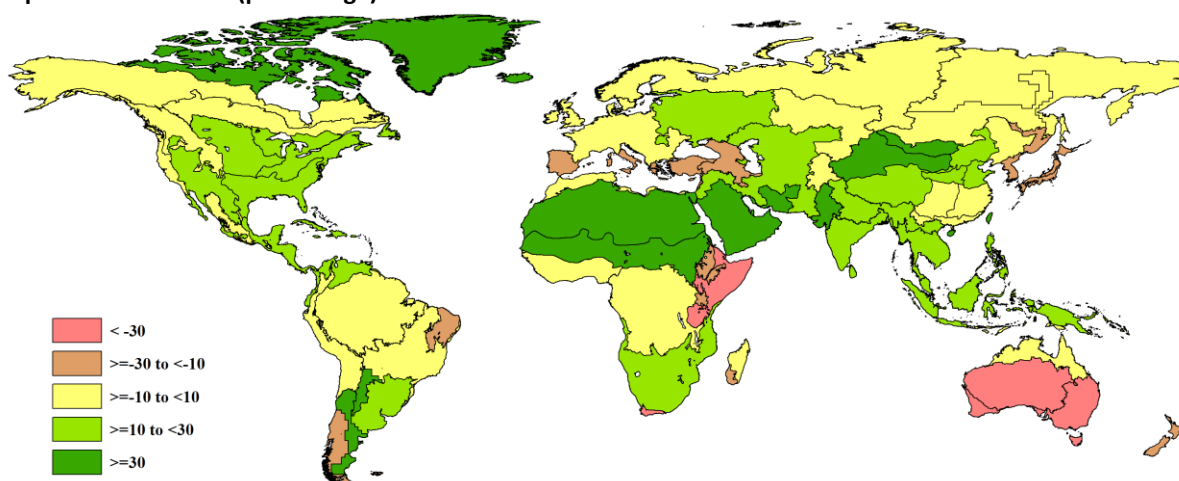
Two more areas deserve mentioning: Southern Africa and the northern Mediterranean. The first includes Mediterranean South Africa (MRU-10, Western Cape, -54% below the expected 167 mm) and southern Madagascar (MRU-06, -15%), while remaining areas of southern Africa (MRU-09) that suffered a serious drought last year are at +12% RAIN. The area has now concluded the maize harvest, the main staple in most of the region. The northern Mediterranean encompasses several MRUs, including Mediterranean Europe and Turkey (MRU-59, RAIN -13%) and the “Caucasus” (MRU-29, RAIN -16%), with the latter including the coastal eastern Mediterranean. It is the northern part of the area identified as B in figure 1.5.

Figure 1.1 confirms a pattern observed in previous bulletins, which is a continent-wide area extending from Senegal to semi-arid central Asia in which precipitation has recently increased over average. The area is shown as H in figure 1.5 and includes also the adjacent areas coded F, G, E and D. The most significant positive departures are observed in the Mongolia region (MRU-47, RAIN +126%) and in Gansu-Xinjiang (MRU-32, +83%), confirming a recent trend of favorable precipitation in central Asia. Other high precipitation areas include MRU-48 (Punjab to Gujarat, +72% with 559 mm instead of 325 mm) in Asia and the Sahel (+35%), which indicates an early start of the rainy season in West Africa.

It is worth noting that most of central, southeast and western Asia had favorable precipitation, sometimes associated with floods (see also Chapter 5, section on disasters).

In Latin America, the semi-arid Southern Cone (MRU- 28) had an increase in rainfall of 83% above average.

Figure 1.1. Global map of April-July 2017 rainfall anomaly (as indicated by the RAIN indicator) by MRU, departure from 15YA (percentage)



1.3 Temperature (TEMP)

Although the largest negative departure over the reporting period occurred in MRU-58 (Ukraine to Ural mountains, TEMP -2.2°C), it was (as mentioned above) mostly tropical and equatorial areas that tended to experience below average TEMP on all continents, starting with Asia. The following areas experienced negative temperature departures close to -1°C (-0.7°C to -1.1°C): Hainan (MRU-33), Southern China (MRU-40), Taiwan (MRU-42), Mainland Southeast Asia (MRU-50), Punjab to Gujarat (MRU-48; also mentioned as one of the areas with very large rainfall excess), and Southwest China (MRU-41) and the Southern Himalayas (MRU-44), both of which were at 0.7°C below average.

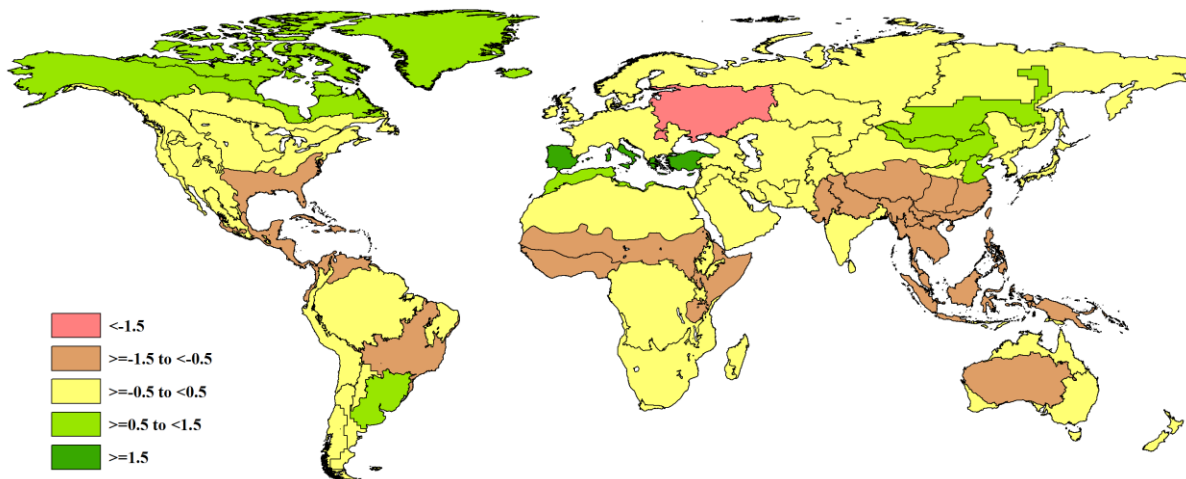
In West Africa, the Sahel (MRU-08, TEMP -0.9°C) must be mentioned, as well as the Gulf of Guinea states (MRU-03, -0.7°C), described also in more detail in Chapter 2 under the West Africa MPZ, and the Horn of Africa. In the Horn of Africa, temperature departure was less marked (-0.5°C).

In Central America and adjacent areas, several MRUs also stand out, starting with the relatively “coldest” area, which encompasses the United States Cotton Belt and the Mexican Coastal Plain (MRU-14, TEMP -0.7°C). In Central America and northern South America (MRU-19) the TEMP departure was -0.6°C , while in central-eastern Brazil (MRU-23) temperatures were closer to average at -0.5°C .

Positive temperature anomalies also occur on all continents, except Oceania. In South America, the major agricultural area of the Pampas stands out with warm temperatures (MRU-26, $+0.6^{\circ}\text{C}$). The most marked warm anomalies, however, affected the Mediterranean basin where rainfall was low (see above). The two affected MRUs here include North Africa (MRU-07; TEMP 0.8°C) and Mediterranean Europe and Turkey (MRU-59), which had the largest positive departure with temperatures as much as 1.6°C above average.

Southeast Brazil (MRU-26, $+0.6^{\circ}\text{C}$) is to be mentioned next, as well as a large block of MRUs in central-eastern Asia, centered around MRU-47 (Mongolia region, TEMP $+1.3^{\circ}\text{C}$), Eastern Central Asia (MRU-52, $+0.9^{\circ}\text{C}$), Inner Mongolia (MRU-35, $+0.8^{\circ}\text{C}$) and Huanghuaihai (MRU-34, $+0.5^{\circ}\text{C}$).

Figure 1.2. Global map of temperature anomaly (as indicated by the TEMP indicator) by country and sub-national areas, departure from 15YA (degrees Celsius)



1.4 Photosynthetically Active Radiation (PAR) and combinations of CWAls

PAR is assessed using the RADPAR indicator. For the current reporting period, the indicator shows an atypically weak correlation with TEMP. Areas with MRUs where the two indicators--RADPAR and TEMP--agree are the following:

- *East Asia*, including MRU-35 (Inner Mongolia, China), MRU-38 (Northeast China), MRU-52 (Eastern Central Asia), MRU-43 (East Asia), MRU-46 (Southern Japan and Korea), and MRU-34 (Huanghuaihai). In this region, TEMP departure was $+0.5^{\circ}\text{C}$ (on average) and RADPAR was $+2\%$ (with values of $+4\%$ in MRU-38 and MRU-46, constituting a record for the reporting period.) Rainfall across the region varied from -30% (MRU-46) to $+17\%$ (MRU-35). (Area A in figure 1.5.)
- *Mediterranean sea area*, covering both the Europe and Turkey MRU (MRU-59) and North Africa (MRU-07). The area's TEMP departure is $+1.2^{\circ}\text{C}$, with a close to average positive RADPAR departure and lower than expected rainfall. (Area B in figure 1.5.)
- *An area covering three American MRUs*, including the Corn Belt (MRU-13), the Caribbean (MRU-20), and the Cotton Belt extending into the northern Mexican coastal plain (MRU-14). Here,

negative departures of both TEMP (-0.6°C on average) and RADPAR (-4%) occur with consistent above average RAIN (+17% on average). (Area C in figure 1.5.)

- *Maritime eastern and southeastern Asia*, with coherent negative departures of TEMP (-0.9°C on average) and RADPAR (a very significant -5%), while RAIN was consistently positive at +24%. Included are MRU-40 (Southern China), MRU-33 (Hainan), MRU-42 (Taiwan), MRU-50 (Southeast Asia mainland), and MRU-49 (Southeast Asia islands). (Area D in figure 1.5).

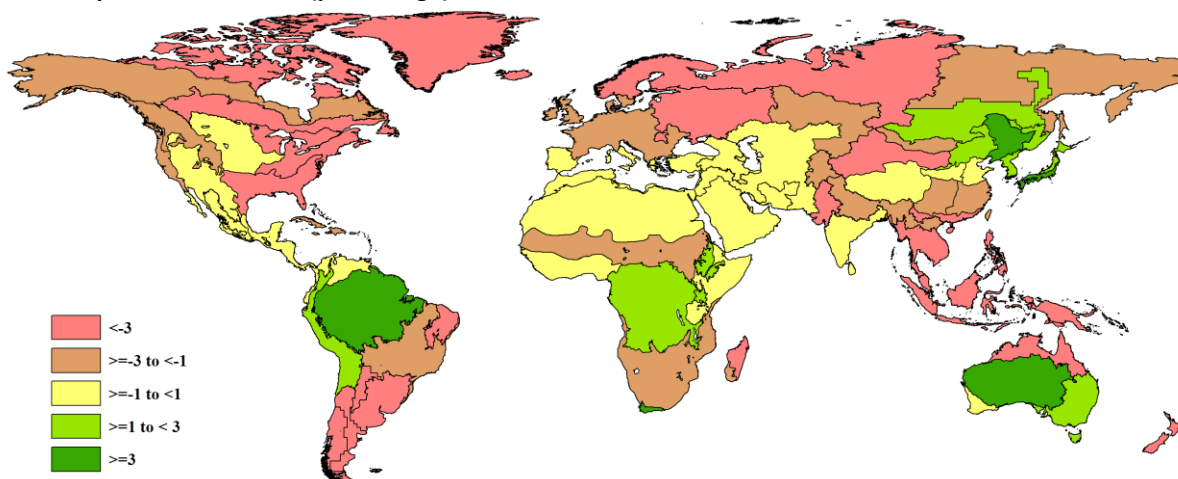
Isolated MRUs where behavior of CWAls, especially TEMP, RADPAR, and RAIN agree include:

- Ukraine to Ural Mountains (MRU-58), with TEMP at -2.2°C, RADPAR at -4%, and RAIN +22%. (Area E in figure 1.5.)
- The Sahel (MRU-08), with respective values for TEMP, RADPAR, and RAIN of -0.9°C, -2%, and +35%. (Area F in figure 1.5.)
- Punjab to Gujarat (MRU-48), with TEMP -0.8°C, RADPAR -2%, and RAIN +72%. (Area G in figure 1.5.)

Finally, New Zealand (MRU-56) stands out with a less classical combination of low rainfall (RAIN, -29%) accompanied by cooler than average temperature (TEMP, -0.3°C) and low sunshine (RADPAR, -9%).

Isolated areas characterized by abnormally low sunshine include central-north Argentina (MRU-25, RADPAR -11%), the Pampas (MRU-26, -7%), and the Brazilian Nordeste (MRU-22), where the end of the growing season had both low sunshine (-6%) and poor rainfall (-26%).

Figure 1.3. Global map of PAR anomaly (as indicated by the RADPAR indicator) by country and sub-national areas, departure from 15YA (percentage)



1.5 Biomass Production Potential (BIOMSS)

Under most circumstances, BIOMSS patterns follow RAIN patterns rather closely, as RAIN tends to vary more than TEMP, the second factor affecting the biomass production potential in the Miami model (see Annex C). The similarity between the BIOMSS (figure 1.4) and RAIN (figure 1.1) map is immediately apparent. However, large differences in the ranking of BIOMSS and RAIN occur in Western Patagonia (MRU-27) and Qinghai-Tibet (MRU-39) due to the combination of high rainfall with unusually cold temperature.

Figure 1.4. Global map of biomass anomaly (as indicated by the BIOMSS indicator) by country and sub-national areas, departure from 5YA (percentage)

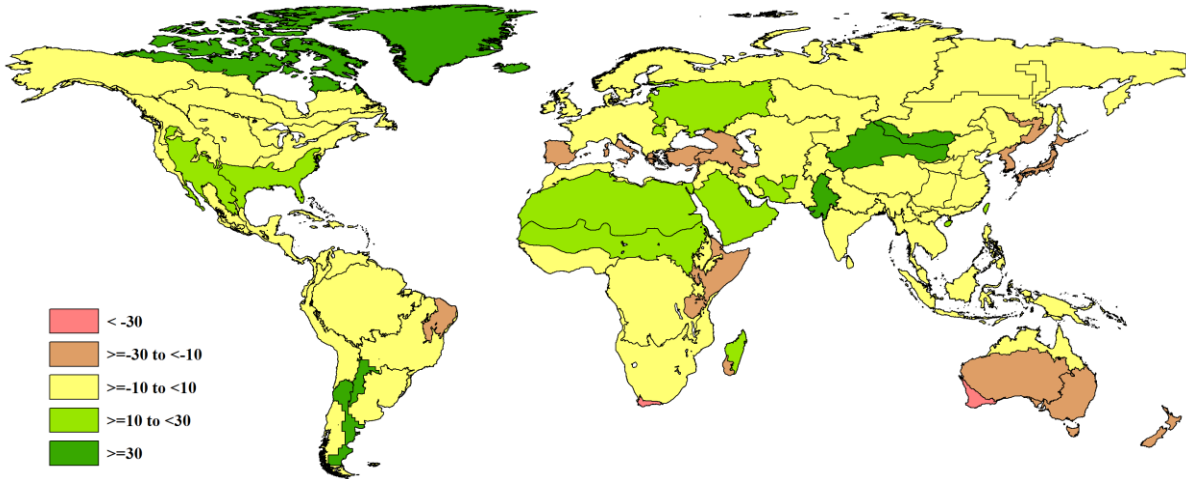
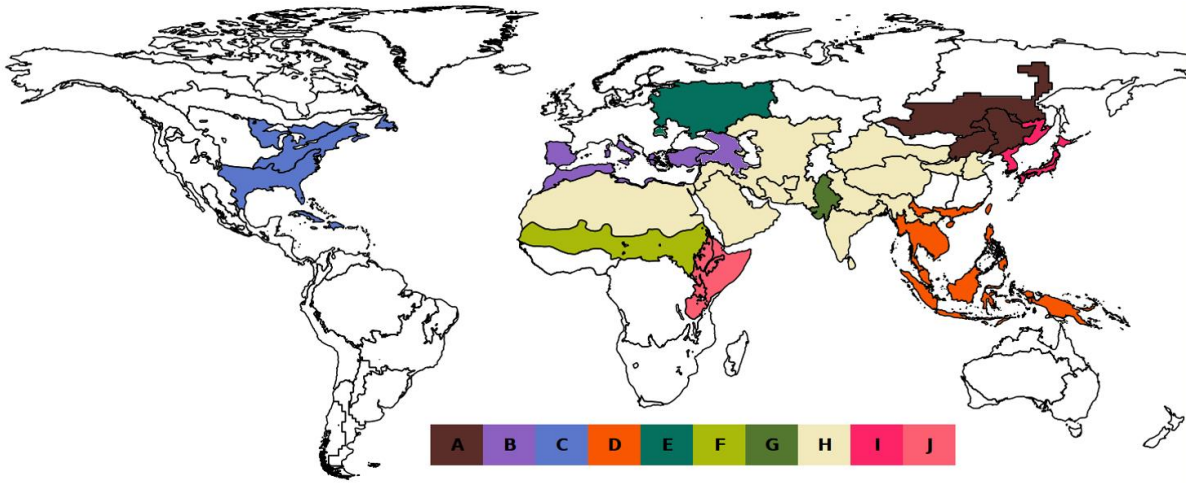


Figure 1.5. Areas of major climatic anomalies



Note: Wet areas are D, E, F, G, and H; dry areas are B, I, and J; sunny and warm: A; dry and warm: B; cool, rainy with low sunshine: C and D. Refer to the text for details.